Increasing the Flexibility of Combined Heat and Power for Wind Power Integration in China: Modeling and Implications

Xinyu Chen, *Student Member, IEEE*, Chongqing Kang, *Senior Member, IEEE*, Mark O'Malley, *Fellow, IEEE*, Qing Xia, *Senior Member, IEEE*, Jianhua Bai, Chun Liu, Rongfu Sun, Weizhou Wang, and Hui Li

***Abstract*—With the largest installed capacity in the world, wind power in China is experiencing a $\sim$ 20% curtailment during operation. The large portion of the generation capacity from inflexible combined heat and power (CHP) is the major barrier for integrating this variable power source. This paper explores opportunities for increasing the flexibility of CHP units using electrical boilers and heat storage tanks for better integration of wind power. A linear model is proposed for the centralized dispatch for integrated energy systems considering both heat and power, with detailed modeling of the charging processes of the heat storage tanks. The model balances heat and power demands in multiple areas and time periods with various energy sources, including CHP, wind power, electrical boilers, and heat storage. The impact of introducing electrical boilers and heat storage systems is examined using a simple test system with characteristics similar to those of the power systems in Northern China. Our results show that both electrical boilers and heat storage tanks can improve the flexibility of CHP units: introducing electrical boilers is more effective at reducing wind curtailment, whereas heat storage tanks save more energy in the energy system as a whole, which reflect a different heating efficiency of the two solutions.**

***Index Terms*—Combined heat and power (CHP), energy system integration, heat storage, wind power.**

I. Introduction

THE installed capacity of wind power in China reached 75 GW in 2012, contributing to 27% of the global wind power capacity [1]. However, the curtailment rate reached 15%-25% in the Northern and Northeastern provinces (where more than 75% of the wind power capacity is installed) in the same year, resulting in a $1.6 billion nationwide economic loss [2].

Combined heat and power (CHP) units with limited operational flexibility are the major limitation for accommodating this variable power source. In provinces experiencing heavy curtailment, CHP accounts for 50%–70% of the generation capacity from fossil fueled units, which operate 120–210 days per year [2]. The power generations from CHP plants are constrained by their heat demand [3]. At off-peak hours in the winter, CHP covers a large portion of the power demand, resulting in a heavy curtailment of wind power.

Introducing additional flexibility in the heating sector could be effective at reconciling the conflict between inflexible CHP operations and the variable generation from wind power. Turning on electrical heat boilers to use the otherwise wasted wind power is a straightforward solution. This solution could be improved by using electrical boilers that are integrated with CHP. This would provide extra flexibility in the heating supply and allow CHP units to further reduce their electricity production.

Heat storage tanks (heat accumulators) represent another solution to increase the flexibility of CHP units for better accommodation of wind power. In these tanks, the interaction of flowing water with the district heating system changes the interior water temperature, providing a lower cost, more environmentally friendly energy storage system than other electricity storage systems (e.g., pumped hydro systems). Such devices could replace part of the heat production from CHP units, correspondingly reducing CHP power production when wind power is abundant. These existing heat storage tanks are mostly utilized in European nations, in particular Denmark [4]. The operational decisions for these heating devices are decentralized and driven by price signals from the power markets.

For power systems, such as those in China, the price of power generation is fixed and wind power is given priority for integration within technical limitations. Under such circumstances, heat storage and electrical boilers have to be dispatched in a centralized scheme. The numerical models of heat storage tanks used by the power producer are computationally extensive and not suitable for large-scale optimization. To quantify the impact of heat storage tanks and electric heat boilers on wind curtailment it is necessary to model their flexibility in system operation. This is the central problem that we will explore in this paper.

Manuscript received January 27, 2014; revised May 06, 2014; accepted August 11, 2014. Date of publication September 29, 2014; date of current version June 16, 2015. This work was supported in part by the National Science Fund for Distinguished Young Scholars under Grant 51325702, the National High Technology Research and Development Program of China (863 Program) under Grant 2011AA05A101, and Research Projects Sponsored by State Grid Corporation of China . Paper no. TPWRS-00019-2014. *(Corresponding author: Chongqing Kang.)*

X. Chen, C. Kang, and Q. Xia are with the State Key Lab of Power Systems, Department of Electrical Engineering, Tsinghua University, Beijing 100084, China (e-mail: cqkang@tsinghua.edu.cn).

M. O'Malley is with the University College Dublin, Dublin 4, Ireland.

J. Bai, C. Liu, R. Sun, W. Wang, and H. Li are with the State Grid Corporation of China, Beijing 100031, China.

Color versions of one or more of the figures in this paper are available online at http://ieeexplore.ieee.org.

Digital Object Identifier 10.1109/TPWRS.2014.2356723

0885-8950 © 2014 IEEE. Personal use is permitted, but republication/redistribution requires IEEE permission.
See http://www.ieee.org/publications_standards/publications/rights/index.html for more information.

Computational fluid dynamic (CFD) models have been used extensively to describe the water temperature distributions within storage tanks [5]–[7]. These numerical models contain up to 1000 variables and are thus not applicable for system-scale dispatch. EnergyPlan [8], among several alternative energy simulation tools summarized in [9], is a comprehensive energy system simulation platform and has been applied to the wind power integration solutions in Jiangsu [10] and Inner Mongolia area [11] in China. The platform has embedded simulation blocks for general heat storage; however, the linear heat loss rate in this model does not specifically describe the charging/discharging processes for heat storage tanks. References [12] and [13] provide a comprehensive model to determine the optimal charging and discharging status for general heat storage devices, which could consider the heat loss in loading and unloading process separately. Reference [13] further extended the optimization from a Co-generation system to a Tri-generation system. References [14], [15] proposed an economic dispatch model that included CHP units, with a comprehensive survey reported in [16], as well as in-depth emission analyzed in [17]; however, the wind and heat storage devices were not considered. References [5] and [18] analyzed the impact of joint operation of heat storage and CHP on power markets, but they did not cover the impacts associated with wind power. References [19]–[21] thoroughly analyzed the impact of heat boilers and heat storage tanks in the power markets of Nordic countries, based on the flexible operation of CHP [22]–[24], but the impact of such heat sources will be different because of the diverse regulatory environment and the incentive for wind power, in particular the operation of electrical boilers is driven by the low price in power market in Nordic countries [19], unnecessarily corresponding to the wind curtailment.

Here, we present a linear model that describes the charging/discharging processes and the interior water temperature changes of a heat storage tank. By modeling the restrictions on the CHP unit, the impact of the electrical boiler and heating storage devices on the flexibility of the CHP unit is studied. Based on our analysis, a dispatch model is developed that optimizes the output from all power and heat production sources to balance the heat and power production for multiple areas at multiple time periods. A small test system containing similar characteristics to that of the power systems in North China is studied. We illustrate the effectiveness of electrical boilers and heat storage devices for reducing wind curtailment. In the context of the previous research, our paper provides the following contributions.

1) We propose a linear control model for heat storage tanks that describes the charging and discharging processes, with relatively few control variables.
2) We propose a linear dispatch model that balances the heat and power demands from large geographical areas with in a centralized dispatch scheme. The model is effective at integrating wind power with CHP and other flexible heat sources in an environment that lacks a price signal.
3) We examine the impact of electrical boilers and heat storage tanks on wind power curtailment in a test system that is similar to that of North China. Our results show that introducing electrical boilers provides a greater improvement in the flexibility of CHP and effectively reduces wind curtailment, whereas the overall energy savings are greater for heat storage systems.

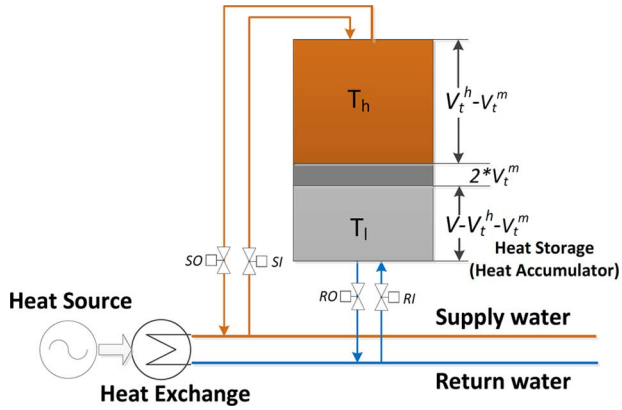

Fig. 1. Interconnection of the heat storage with the district heating network and its interior stratification.

The linear control model of the heat storage is presented in Section II. The constraints of the CHP unit and the corresponding changes that occur when flexible heat sources are introduced are formulated in Section III. A dispatch model considering the CHP units, the heat accumulators, electrical boilers and the wind power required to meet heat and power balance demands is proposed in Section IV. The impact of introducing electrical boilers and heat storage devices on wind curtailment and fuel use are illustrated by a case study in Section V. Conclusions are presented in Section VI.

II. Control Model for Heat Storage

Here, we describe the structure and operation of the heat storage tank. The mathematical modeling of the energy balance within the storage tank is formulated based on the stratification of the interior water temperature. We also propose a linear control model for large scale optimization.

A. Description of Heat Storage Tank

The typical stainless steel heat storage tank in Europe is a cylinder with a height of 20–30 meters and a width of 3–5 meters, containing 600–1000 m^3 of water. The walls are composed from the inside to the outside of stainless steel, concrete, and a layer of heat insulation material. The tank is well insulated, and the daily heat loss through the walls is less than 0.7% of the total stored energy[1] and thus can be ignored.

The connection between the heat storage tank and the district heating system is shown in Fig. 1. The water inlet SI and outlet SO at the top of the tank are both linked to the high-temperature water supply in the heating district, whereas the water inlet RI and outlet RO on the bottom of the tank are connected to the return water pipe containing low temperature water.

The water temperature in the tank is stratified into three temperature layers. The water temperature in the upper layer

[1][Online]. Available: http://www.energinet.dk/SiteCollectionDocuments/Danske%20dokumenter/Forskning/Technology_data_for_energy_plants.pdf

is equal to the water temperature in the supply pipe from the heating district, denoted as $\mathrm{T_h}$. The water temperature in the lowest layer is the same as the water temperature in the return network, denoted as $\mathrm{T_1}$. The water temperature in the middle layer degrades gradually from the upper layer to the lower layer, forming a mixed temperature zone.

During the charging process, the SI is open to inject the high-temperature water from the supply network and the RO is open to let low temperature water flow out through the return water pipe. The upper layer expands and the mixing layer moves downwards. During the discharging process, the RI and SO are open so that the high-temperature water in the tank is injected into the supply network. The injected water is replaced by low-temperature water from the return network. The lower layer expands, and the mixing layer moves upwards.

The mixing temperature zone expands during the charging and discharging processes, as the heat flows continually from the high-temperature region to the low-temperature region until the tank is either fully charged or fully discharged. The water in this zone cannot be reinjected to the supply water pipe and thus causes the major energy loss during the charging/discharging process. Energy loss is modeled in detail below.

B. Dispatch Model

1) Mathematical Modeling of the System: CDF models have been applied to the heat storage tanks to simulate their operation and analyze their heat loss [4]–[6]. However, this model contains over 1000 variables for each heat accumulator and is thus not applicable for large-scale optimization problems. The model in [12] and [13] is comprehensive to optimize the charging and discharging process of heat storage devices. In the model, charging rate and discharging rate are modeled separately so that heat loss rate associated with both process could be differentiated. In this paper, a simplified linear dispatch model for the system level operation is proposed based on the model in [12], [13] in view of the stratification characteristic described in the CDF model.

Suppose the total volume of the water tank is V, the volume of the hot water at time t is V_t^h, and the volume of the water in the mixing region at time t is $2 \cdot V_t^m$, as shown in Fig. 1. The total heat of the system can be expressed by

$$Q_t = c\rho(V_t^h - V_t^m)T_h + c\rho(V - V_t^h - V_t^m)T_l + c\rho V_t^m(T_h + T_l) \quad (1)$$

where c is the heat capacity of the water and ρ is the water density.

In the discharge process, the volume of the hot water is replaced by the cold water. The net energy released to the district heating system is proportional to the temperature difference between the supply water and the return water. As the water in the mixed layer would reduce the temperature in the heating network if reinjected, it is not to be used in the discharging process. The overall available heat Q_t^{av} to be released to the heating network depends only on the volume and heat content of the hot water, as shown in

$$Q_t^{\mathrm{av}} = c\rho(V_t^h - V_t^m)(T_h - T_l). \quad (2)$$

The energy loss $Q_{\mathrm{loss}}(t)$ in the thermal storage tank results from the volume of hot water replaced by the mixing layer, as shown in

$$Q_{\mathrm{loss}}(t) = c\rho V_t^m(T_h - T_l). \quad (3)$$

In the charging and discharging processes, the mixing layer becomes thicker over time, as the heat flows constantly from the hot water to the cold water. When the charging/discharging processes finish, the mixing layer stops expanding. In this paper, we assume that the volume of such a layer expands linearly over time during the charging/discharging process. As the expansion rate decreases when the layer get thicker, the linear expansion assumption would cause less than 5% of difference on the availability of heat energy in the storage tank for the typical charging cycle [4]. The change in volume of the temperature mixing layer over time is expressed as

$$V_t^m - V_{t-1}^m = \begin{cases} 0, & V_t^h = 0 \\ \eta\Delta t, & 0 < V_t^h < V \\ 0, & V_t^h = V \end{cases} \quad (4)$$

where η is the expansion rate of the mixing layer, which is dependent on the temperature difference and performance of the water stratification. The time duration between consecutive time intervals is denoted by Δt.

2) Dispatch Model of the Storage Tank: Based on our previous analysis and some assumptions, we propose a control model that can be used to determine when and how to charge or discharge the tank. In the model, the decision variable is the heat released to the heating network at each time period. The available heat in the tank and the corresponding heat loss are changed correspondingly. The relationships between the charging/discharging rate of the tank and the available heat and heating energy loss are formulated in a linear fashion.

The increment of available heat energy at time t in the $\mathrm{i^{th}}$ heat storage tank is

$$Q_{it}^{\mathrm{av}} - Q_{i(t-1)}^{\mathrm{av}} = -q_{it}^s - \Delta Q_{it}^{loss} \quad (5)$$

where q_{it}^s is the heat released to the heating network at time t from ith heat storage tank. The variable is negative when the tank is in the charging state. The index i represents the sequence of elements within each category of energy sources (such as heat storage, CHP, and other heating elements) in this paper hereafter.

The increased energy loss at time t due to the mixing of hot and cold water is denoted by $\Delta Q_{it}^{\mathrm{loss}}$, which is determined by (3) and (4). The following equations use a slack variable to formulate the energy loss in a linear form:

$$\begin{aligned} \Delta Q_{it}^{\mathrm{loss}} &= Q_{it}^{\mathrm{loss}} - Q_{i(t-1)}^{\mathrm{loss}} \\ &= \eta \cdot \Delta t - \varphi_{it} \quad (6) \\ 0 &\le Q_{it}^{\mathrm{av}} \pm Q_{it}^{\mathrm{loss}} \\ &\le c\rho V_i(T_h - T_l). \quad (7) \end{aligned}$$

In (6), φ_{it} is the slack variable of the energy equation that is penalized in the objective function of dispatch model later in Section IV. If $0 < V_t^h < \overline{V}$, φ_{it} is set to zero to avoid the

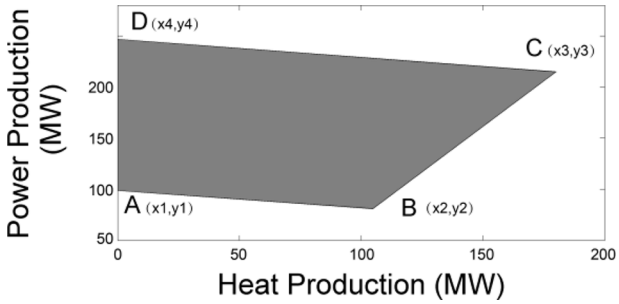

Fig. 2. Feasible operational area of heat and power production in CHP unit.

penalty in the objective function. When the tank is either fully charged ($V_t^h = V$) or fully discharged ($V_t^h = 0$), (7) reaches either the upper or lower limit, and the slack variable will set $\Delta Q_{it}^{\text{loss}}$ to zero. In both cases, (6) and (7) produce the same effect as in the nonlinear equation (4).

The volume limit of the tank and the charging/discharging speed are

$$0 \le Q_{it}^{\text{av}} \le c\rho V_i(T_h - T_l) \tag{8}$$

$$|q_{it}^s| \le \Delta Q_i^{\max} \tag{9}$$

where $\Delta Q_i^{\max}$ is the maximum charging and discharging rate, which is determined by the characteristics of the tank.

III. Modeling the CHP Plant

Here, a convex combination method is used to present the heat and power coupling of the CHP unit. The changes in the feasible operational area of the CHP when the electrical boiler and heat storage tank are introduced are presented.

A. Mathematical Formulation of the Feasible Operation Area

The feasible operating area for heat and electrical power production in the combined heat and power plant is shown in Fig. 2. The boundaries of AD, AB, BC, and CD represent the minimum limit of steam injection, the maximum heat rate, the maximum limit of fuel injection, and the maximum limit of power output, respectively. The electricity and heat production of the corner point i (intersection of the boundaries) is defined as (x_i^k, y_i^k).

The heat and power production of the ith CHP at time t are coupled. These parameters have to stay within the feasible operation area. As any point within the area can be represented by the convex combination of corner points [14], the relationship between power production, heat production and the coordinates of the corner points are expressed by

$$\begin{aligned} p_{it}^c &= \sum_{k=1}^{M_i} \alpha_{it}^k x_i^k \\ q_{it}^c &= \sum_{k=1}^{M_i} \alpha_{it}^k y_i^k \end{aligned} \tag{10}$$

where M_i is the total number of corner points for the ith CHP and the combination coefficient α_{it}^k satisfy the following equations:

$$0 \le \alpha_{it}^k \le 1 \qquad \forall i, t, k \tag{11}$$

$$\sum_{k=1}^{M_i} \alpha_{it}^k = 1 \qquad \forall i, t. \tag{12}$$

The fuel cost of a CHP power plant is generally defined as a quadratic function of the electrical power and heat output, including the product of the power and heat production [10], shown as in (13).

$$FC = \mu_0 + \mu_1 \cdot p + \mu_2 \cdot q + \mu_3 \cdot p^2 + \mu_4 \cdot q^2 + \mu_5 \cdot pq. \tag{13}$$

A linear cost function employing the convex combination is introduced to approximate the quadratic cost function in (13). The cost can be expressed by

$$C_{it}^c = \min \sum_{k=1}^{M_i} \alpha_{it}^k c_i^k \tag{14}$$

where c_i^k is the corresponding fuel cost for each corner point of unit i. For a given status of heat and power production, multiple sub-sets of corner points can be chosen to represent the status of power and heat production, but the "min" used in (14) ensures the cost for each status is unique. The cost function in (14) is convex.

B. Expansion of the Feasible Operational Area by Introducing Heat Storage and Electrical Boilers

Introducing heat storage tanks and heat boilers to operate in parallel with the CHP unit will expand the overall heat and power production area. The equivalent heat and power production from the ith CHP unit when coupled with electrical boilers and/or heat storage devices are expressed as

$$\begin{aligned} p'_{it} &= p_{it}^c - p_{gt}^{eb} \\ q'_{it} &= q_{it}^c + q_{gt}^{eb} + q_{rt}^s \end{aligned} \tag{15}$$

where p'_{it} and q'_{it} represent the equivalent heat and power production of the ith CHP unit, respectively, when combined with the electrical boiler and/or the heat storage tank, if any. The electricity used in the gth electrical boiler at time t is denoted by p_{it}^{eb}, which produces q_{gt}^{eb} at a conversion efficiency of η_g^{eb}. q_{rt}^s denotes the heat output from the rth heat storage devices heat storage at time t.

The expanded boundaries for the overall heat and power production of a typical 300-MW CHP unit when coupled to a 50-MW electrical boiler and/or a 50-MW heat storage device are shown in Fig. 3. The grey areas show the boundaries coupled with flexible heat sources, whereas the dark areas represent that of the CHP.

Adding an electrical boiler expands the maximum overall production level of heat, whereas the lower output level of electricity production decreases, because part of the electricity generated from CHP is used in electrical boiler to produce heat. The upper boundary remains unchanged, which reflects

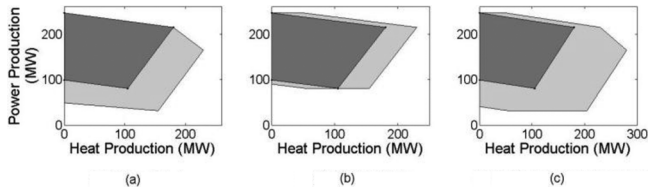

Fig. 3. Power production from each CHP unit when combined with flexible heat sources.

the status that CHP is producing at maximum capacity and the electrical boiler is turned off. The feasible operating area is thus expanded to the lower right region, as shown in Fig. 3(a).

When coupled to heat storage, the possible heat output of the CHP unit expands by ± 50 MW at any given power output level. The lower left boundary in Fig. 3(b) shifts leftwards when heat storage acts as a heat load, and the lower right boundary shifts rightwards when it acts as heat provider. The increased flexibility of adjusting the heating output allows the CHP unit to reach lower power output at a given heat production level, as shown in Fig. 3(b). Using both the electrical boiler and the heat storage device dramatically expands the maximum heating production level, but the expansion of the lower limit is marginal compared to only using the electrical boiler, as shown in Fig. 3(c).

It is also noteworthy that adding heat storage increases the maximum limit of power production of the CHP unit marginally in the short term in Fig. 3(b) and (c), as more energy in the CHP unit can be used to generate electricity when part of the heat load shifts from CHP to heat storage. Thus, heat storage can also contribute to the system reserves, although it is not directly linked to electricity production.

IV. Dispatch Model for Heat and Power Production

Here, a joint dispatch model that considers the CHP unit, wind power, the heat storage tank, and the electrical boiler is proposed to meet the electricity and space heating demands in heating districts. Wind power is given priority for integration. The overall energy cost is minimized in the model. The proposed model is linear, requiring the operational region of CHP to be convex.

A. Decision Variables

The decision variables include energy generation for both power and heat generation for each unit at every time period, the power consumption in electrical boilers, extra variables of CHP described in (10), as well as the variables related to the interior status of heat storage tanks (volume of hot water and energy loss in Section II) p^e_{it} and p^w_{it} represent the power production from each conventional power plant and each wind farm at time t, respectively. p^c_{it} and q^c_{it} represent the power and heat production in the CHP unit as in (10), respectively. $Q^h_{i,t}$, $q^s_{i,t}$ and $Q^{eb}_{i,t}$ represent the heat output from each heat boiler, the heat storage tank and the electrical heat boiler at time t, respectively. Other variables associated with the status of the CHP units and the heat storage devices are also included in the model.

B. Objective Function

The proposed model is designed to minimize the wind power curtailment, as well as the fuel consumption. The objective function includes the total fuel cost, the penalties on curtailment of wind power, and the slack variables. The penalty of wind curtailment is included because of the renewable energy law mandate the priority of wind power integration within the technical limit. The fuel cost considered in the objective includes the fuel cost in each power plant, the conventional heating plant and the combined heat and power plant, according to

$$\min f = \sum_{t=1}^{n}\sum_{i=1}^{N_p} C^p_{it} + \sum_{t=1}^{n}\sum_{i=1}^{N_q} C^q_{it} + \sum_{t=1}^{n}\sum_{i=1}^{N_c} C^c_{it} + C_W + \xi \tag{16}$$

where N_p, N_q, and N_c are the number of power plants, heating plants and combined heat and power plants, respectively. C_W is the penalty term for wind curtailment. The penalty term on the slack variables is denoted by ξ. C^c_{it} is decided according to (14), while the fuel cost from power plant C^p_{it} and the fuel cost from the heating plant are linearly dependent on the fuel consumption. C_W and ξ are determined from

$$C_W = \theta_1 \cdot \sum_{t=1}^{n}\sum_{i=1}^{N_w} (\bar{P}^w_{it} - p^w_{it}) \tag{17}$$

$$\xi = \theta_2 \cdot \sum_{t=1}^{n}\sum_{i=1}^{N_s} \varphi_{it} \tag{18}$$

where θ_1, θ_2 are respectively the penalty factors for wind curtailment and slack variable for heat storage tank. $\overline{P}^w_{it}$ is the available wind power of wind farm i at time t and p^w_{it} is the actual power output in wind farm i at time t. N_w and N_s are respectively the number of wind farms and heat storage tanks. φ_{it} is from (6).

C. Constraints

1) Power Balance: The system load equals the sum of the power output from all of the power units, the CHP plants and the wind farms, subtracting the power demand from the electrical boilers according to

$$\sum_{i=1}^{N_p} p^e_{it} + \sum_{i=1}^{N_c} p^c_{it} + \sum_{i=1}^{N_w} p^w_{it} - \sum_{i=1}^{N_{eb}} p^{eb}_{it} = P_t \quad \forall t \tag{19}$$

where N_{eb} is the total number of electrical boilers. P_i is the system load at time t.

2) Zonal Heat Balance: Due to the limited interconnections of the district heating zones, the heating demand is balanced separately within each heating district. Suppose we have N heating districts and M heating sources. The connection matrix $\mathbf{A}_{MN}$ is defined as

$$\mathbf{A}_{MN} = \begin{bmatrix} a_{11} & a_{12} & \cdots & a_{1N} \\ a_{21} & a_{22} & & \\ \vdots & & \ddots & \\ a_{M1} & & & a_{MN} \end{bmatrix} \tag{20}$$

where a_{ij} indicates the connection of the ith heating element to the jth heating district. When $a_{ij} = 1$, the ith heating element

is connected to the jth heating district. When $a_{ij} = 0$, the other situation occurs. Let $a^h_{ij}, a^c_{ij}, a^{eb}_{ij}$ and a^s_{ij} represent the elements in the connection matrix for the heat boilers, the CHP unit, the electrical boiler and the heat storage devices, respectively. The zonal heating balance can then be written as

$$\sum_{i=1}^{N_h} a^h_{ij} Q^h_{it} + \sum_{i=1}^{N_c} a^c_{ij} q^c_{it} + \sum_{i=1}^{N_e} a^{eb}_{ij} Q^{eb}_{it} + \sum_{i=1}^{N_s} a^s_{ij} q^s_{it} = Q_{jt} \quad (21)$$

where Q_{jt} is the heating demand in heating district j at time t, $q^s_{i,t}$ is the heat released from heating storage tank i at time t, and $Q^{eb}_{i,t}$ is the heat generated from heating electrical boiler i at time t, which is linearly related to its electricity consumption by a constant converting efficiency η^{eb}_i according to

$$Q^{eb}_{it} = \eta^{eb}_i \cdot p^{eb}_{it}. \quad (22)$$

3) Constraints on the CHP Unit and the Heat Storage Tanks: The constraints related to the interior variables described in Sections II and III are included in the model. For the CHP units, the constraints on heat and power production in (10)–(12), and (14) are included in the model. For the heat storage tanks, the limitations on the internal status are described in (5)–(9). The energy balance constraint is included for every heating storage tank so that the available heat of the last time period equals to that in the first time period.

Other constraints related to maximum and minimum generation limits, network constraints as well as ramping rate are also included in the model. The maximum and minimum generation limits applies to thermal power units, wind power heat boilers as well as electrical boilers. The network constraint uses the power distribution shift factor, based on dc power flow. Ramping constraints on CHP units employ the form as in [20].

In summary, the model consists of system constraints from (19)–(22), constraints on the CHP unit from (10)–(12) and (14), constraints on the heat storage tank from (5)–(9), and other regular constraints described in the previous paragraph.

V. Case Study

A simple test system is used to simulate the joint dispatch of wind power, the CHP units and the conventional units. The heat storage and electrical boilers are set as optional flexible heat sources in different scenarios. The impact of introducing different electric boilers and heat storage is analyzed based on comparisons of wind curtailment and fuel reduction.

A. Test System and Scenarios

1) 6-Bus Test System: A 6-bus system [26], [27] is used to illustrate the effect and impact of electrical boilers and heat storage systems, as shown in Fig. 4. The system has two conventional units (G_1 and G_2), two CHP units, and one wind farm (W_1). The Load is equally distributed between buses 3 and 6. The two CHP units serve two independent heating districts. CHP-1 along with a 50-MW conventional coal-fired boiler serves heating district I, while CHP-2 serves heating district II.

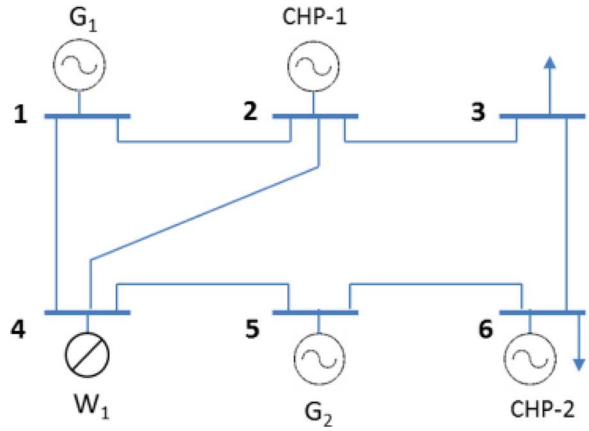

Fig. 4. Modified 6-bus test system.

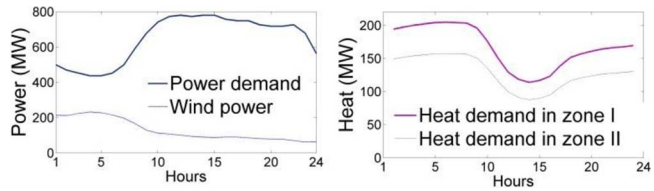

Fig. 5. Power and heat demand as well as wind power output.

The hourly power demand, wind generation, and heating demand for the two heating districts are shown in Fig. 5. The hourly load data is derived from the Illinois Institute of Technology (IIT) 6-bus test data system in [26]. The hourly load is then multiplied by a factor of 3 to match the installed generation. The minimal power demand is around 400 MW, corresponding to 50% of the peak power demand. The hourly capacity factor for wind power is derived from the simulated wind power output [27] in the Hebei province of China on November 11, 2011, based on hourly meteorological data in [28]. It is negatively correlated with the power demand. The wind production accounts for 20% of the total electricity demand.

The parameters for each transmission line are derived from [26]. The power flow limits for transmission lines are also multiplied by a factor of 3 compared with the original data, to be consistent with the power demand. The characteristics of the CHP unit and the conventional heat boilers are based on the data from [25]. The costs are consistent with Chinese statistics for power plant efficiency [31]. The fuel costs for each type of unit are summarized in the Appendix.

2) Scenarios: The heating demand in district II is assumed to be served by different combinations of heating sources in four different scenarios, while CHP-1 and the 50-MW coal-fired boiler serve for heating district I in all scenarios. In addition to CHP-2, a 50 MW electrical boiler and a 50-MW heat storage device with a maximum heat storage capacity of 500 MW are considered as optional heat sources. Scenario S0, the business as usual (BAU) scenario, uses CHP-2 as the only heat source for heating district II. Scenarios S1 and S2 introduce the electrical boiler and the heat storage tank, respectively, as additional heat sources. S3 introduces both the electrical boiler and the heat

	No E-boiler	50MW E-boiler
No H-storage	**S0**(BAU)	**S1**(E-boiler)
50MW H-storage	**S2**(H-storage)	**S3**(both)

Fig. 6. Different scenarios for the heating sources in heating district II along with the CHP unit.

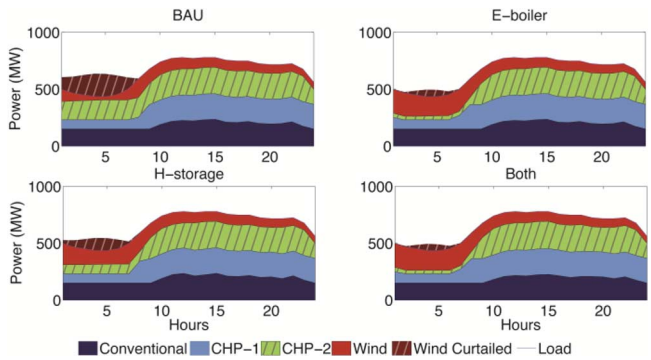

Fig. 7. Power balances for each scenario.

storage tank. The combination of heating sources for each scenario is shown in Fig. 6.

B. Results

1) Hourly Power Balance: The hourly power output for each type of power generation unit for each scenario is shown in Fig. 7. Wind is largely curtailed in the off-peak hours due to the minimal load problem in the BAU scenario. The minimal output for CHP-2 in the second heating zone is constrained to be around 150 MW in the off-peak hours by the heating supply, because no alternative heating source is introduced. At peaking hours when heat demand is lower and power demand is higher, CHP has more flexibility and wind is easier to be integrated.

The 50-MW electrical boiler in S1 decreases the equivalent power output of heating zone II to around 50 MW, creating an extra 150-MW margin for the wind power in the off-peak period. Similarly, the minimal output level for CHP-2 deceases to 100 MW in S3, also decreasing the curtailment rate of the wind power. Combining the heat boiler and the heat storage device does not further lower the output limit of CHP-2, compared to the S1 scenario. The corresponding effect on reducing the wind curtailment is also similar to the S1 scenario.

2) Operating Points for CHP-2 for Joint Production of Power and Heat: The interior status of CHP-2 at off-peak hours with significant wind power curtailment (1 a.m. to 9 a.m.) is illustrated in Fig. 8. Given the heat demand around 150 MW and the constraints on the operational area, the power output can at most be reduced to around 150 MW in the BAU scenario.

Adding additional flexible heat sources in S1–S3 relieves the real-time balance of heat production from CHP and heat demand. Thus, the actual power production from CHP reduces

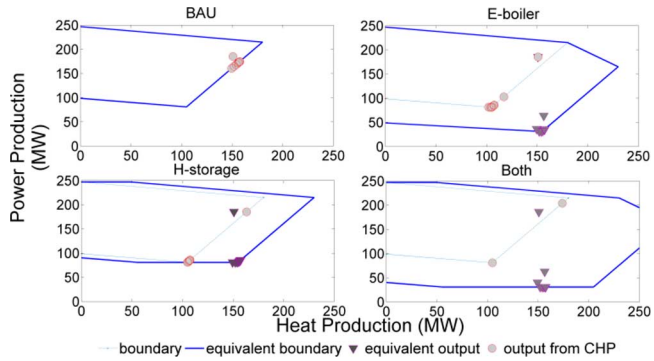

Fig. 8. Equivalent operating points of the CHP unit with different heating sources.

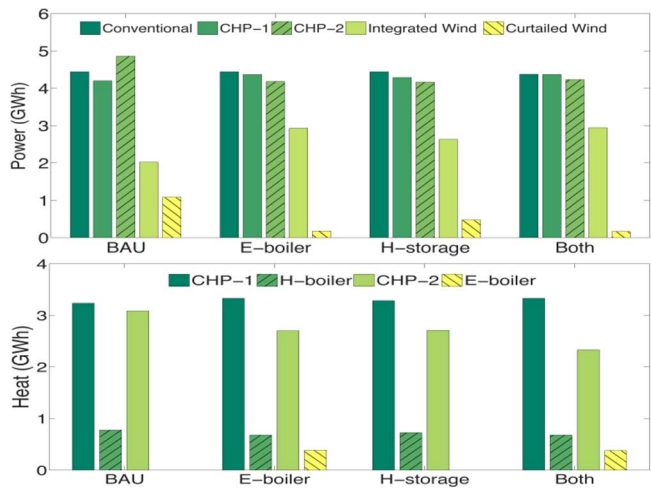

Fig. 9. Power and heat production for each unit.

to its lowest point (90 MW) to be replaced by the otherwise curtailed wind power, as shown in Fig. 8. The insufficient heat supply is made up by the electrical boiler in S1, the heat storage tank in S2, and both heating sources in S3. Heat released from the storage tank is reloaded later in the peaking hours by extra heat production from CHP, as illustrated in Appendix B. Considering the electricity consumption by the electrical boiler, the equivalent minimum generation level attainable is less than 50 MW.

Using both the heat storage device and the electrical boilers allows the operating points for CHP to move to the lowest power production level. However, the marginal benefit of reducing the power production is not significant compared with the S1 scenario (E-boiler).

3) Power/Heat Production: The power and heat production for each unit are summarized in Fig. 9. The curtailment in the BAU scenario reached 34.9% of the total wind power production. The CHP-2 generates 4.85 GWh of electricity, which is the highest of all four scenarios.

When introducing the electrical boiler in S1, the curtailment rate of wind power decreases to 5.6% of the total wind power production, along with a 677-MW decrease in the electricity generation from CHP-2. Given that the electricity used in the electrical boiler is 384 MWh and reduced wind curtailment in S1 compared with BAU is 907 MWh, consuming 1 MWh of

TABLE I
COAL USE FOR EACH TYPE OF ENERGY SOURCE FOR DIFFERENT SCENARIOS

Coal use (Tce)	S0 (BAU)	S1 (E-boiler)	S2 (H-storage)	S3 (Both)
Conventional unit	2198.6	2198.6	2198.7	2165.3
CHP	2377.5	2277.9	2260.2	2242.9
Coal-fired boiler	119.8	105.1	112.1	105.1
Total	4695.8	4581.5	4570.9	4513.2

electricity in electrical boilers will accommodate an extra 2.4 MWh of wind, compared with the BAU scenario, which largely benefits from the increased flexibility of the CHP unit.

Introducing heat storage also largely reduces the wind curtailment rate to 15.3%, accommodating an extra 607 MWh of wind power. The power production drops by 697 MWh. Little improvement for wind curtailment is achieved by combining heat storage with the electrical boiler, compared with the electrical boiler scenario in S1, as the power output from CHP has already at a minimum.

Using different heating measurements in heating district II also affects the production level of different heat sources in heating district I, as shown in the lower part of Fig. 9. In the BAU scenario, the ineffective heat production from the coal-fired boilers must increase so that the electricity production of CHP-1 can decrease to reduce the heavily curtailed wind. Such situations can be avoided when introducing heat sources such as heat storage tanks, demonstrating the interaction across the energy system and potential for benefits of integrated solution.

4) Primary Energy Consumptions: Although the electrical boiler solution is more effective at reducing wind curtailment, the savings in primary energy consumption favor using the heat storage solution, as shown in Table I. The total primary energy consumption in S1 (E-boiler scenario) and S2 (H-storage scenario) is reduced by 114 and 125 tons of standard coal equivalent (Tce), respectively, compared with the BAU scenario. In the contrast, the wind curtailment is reduced by 907 and 607 MWh in S1 and S2 scenarios, respectively. Thus, integrating 1 MWh of wind power can save 0.13 tons of coal for the electrical boiler solution;, whereas using every MWh of curtailed wind power can replace 0.20 tons of coal, compared with the BAU scenario. The difference in primary energy savings between the two solutions generally reflects the low heating efficiency of the electrical boiler.

Using both flexible heat sources can achieve the lowest primary energy consumption among all four scenarios, although the effectiveness of wind curtailment reduction is similar to S1. Harnessing every MWh of curtailed wind power can save 0.19 tons of coal, making scenario S3 the most effective solution in terms of energy savings. The approximation of cost in CHP unit based on convex combination in (14) will marginally increase the primary energy consumptions in all scenarios, but does not affect the comparison between scenarios.

5) Financial Payback: We assume the coal price in China is \$100/ton and the investment cost of an electrical boiler and heat storage are \$0.067 million/MW [31] and \$0.16 million/MW [4], respectively. Previous results suggest that using every MWh of electricity in electrical boilers can reduce 2.3 MWh of wind power curtailment, and integrating 1 MWh of additional wind power could save 0.13 ton of coal via electrical boiler solution. For the illustrative case study here (CHP consists 60% of thermal generation capacity, and wind power constitutes 20% of the power demand) and based on a single day representation of the entire year, an approximation of the financial payback over time shows that the investment cost covers 2427 h of electrical boiler operation. In the Northern part of China, this investment would be repaid in at most four years, assuming the heating period is 150 days and the electrical boiler operates 4 h per day. A similar analysis suggests the investment of heat storage tanks could be covered within two years. The financial payback in the studied system is more optimistic than studies in Nordic countries [19], mainly due to the inflexible conventional power generation and the fixed price of wind power.

The investment payback time is affected by the ambient temperature of the heating space, the wind power output, the generation mix and the network connection. Sensitivity analysis on heating demands is shown in Appendix C. Curtailment rate and effectiveness of flexible heat sources are all affected by this factor. The detailed investment analysis incorporating the hourly load temperature, wind power, and actual power system data can be studied in future publications.

VI. CONCLUSION

In this paper, a linear centralized dispatch model that balances power and heat demands in multiple areas at multiple time periods with energy sources including CHP, wind power, electrical boilers, and heat storage devices is proposed. The proposed control model for the heat storage tank is effective at simulating the charging/discharging process with a linear formulation. When integrating wind power and CHP by introducing electrical boilers and heat storage tanks in heating season, the curtailment rate can be largely reduced, because the flexibility of CHP is improved and its minimum power output is reduced. Compared with different flexible heat source solutions, electrical boilers are more effective at reducing wind curtailment. Heat storage tanks, however, can provide more saving by reducing every kWh of wind curtailment. Combining both solutions can achieve the lowest overall primary energy consumption in the system. An indicative calculation of the financial payback time shows the economic feasibility of the test system for a single day; however, a more accurate analysis of the actual energy system will be studied in future work. Also, other alternative solutions such as bypass the steam for heat production in CHP, and investing in heat pumps as additional heat sources will be included in the future work. A synergizing air-conditioner with wind power will also be analyzed in future work.

APPENDIX A
CHARACTERISTICS OF CHP UNITS

The two CHP units in the test system share the same characteristic as in Table II, where Tce (ton of coal equivalent) is an energy unit adopted in the statistical book in China, defined as energy generated by burning one ton of coal, equivalent to 27.78 MMBTU.

The averaged generation cost of a coal-fired unit and heat boiler are 0.330 Tce/MWh_electricity and 0.154 Tce/MWh_heat, respectively.

TABLE II
FEASIBLE OPERATION AREA AND CORRESPONDING COST

Corner point	Heat production (MW)	Power production (MW)	Coal use (Tce)
A	0	98.8	27.2
B	104.8	81	32.2
C	180	215	58.4
D	0	247	42.5

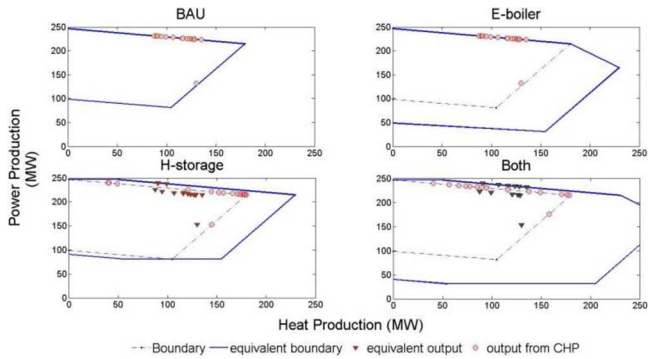

Fig. 10. Equivalent operating points of the CHP unit with different heating sources at peaking hours.

APPENDIX B
PROFILE OF ENERGY OUTPUT FROM CHP UNIT IN OTHER TIME PERIODS

Fig. 10 illustrates the status of CHP devices for each scenario on the time intervals (10 a.m.-12 a.m.). The round dots indicate the operating points for CHP itself, whereas the triangle points indicate the overall energy production when consider electrical boiler/heat storage.

The upper right figure (entitled E-boiler) shows the operating points in the peaking period when combined with electrical boiler. The operating points are not affected by introducing electrical boiler, which indicates the electrical boiler is only used when wind power is at surplus during off-peak hours. On the contrast, the lower left figure (entitled H-storage) illustrates the operating points of CHP when combined with heat storage. The overall heat production is less than the actual heat output from CHP, as the heat storage has to be charged during the peaking hours to keep its energy balance.

APPENDIX C
SENSITIVITY ANALYSIS ON THE LEVEL OF HEAT DEMAND

Sensitivity analysis on different level of heat demand is given to analysis the effectiveness of different heat sources on wind power integration in such CHP dominated system.

The heat demands in both heating sector vary from 20% to 100% of the original heating demand level. The corresponding wind power curtailment rates with different combination of flexible heat sources are shown in Fig. 11. The wind curtailment rate starts from $\sim$ 20% at 20% original heating demand, touches bottom at 60% of the heating demand, and shoots up to 35% when supplying 100% of the original heating demand.

Adding electrical boiler will largely reduce the curtailment rate when heat demand is high, while the effectiveness reduces remarkably when supplying 20% of original heat demand level.

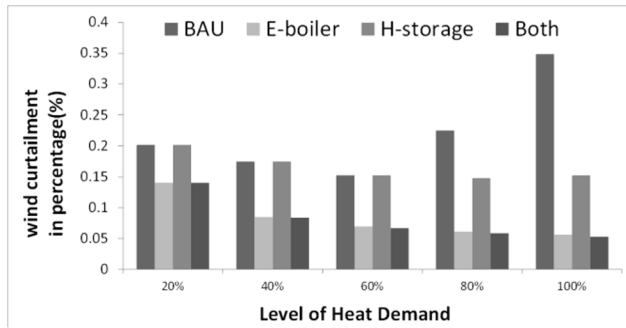

Fig. 11. Wind curtailment rates associated with different scenarios under different level of heat demand.

The effectiveness of heat storage largely diminished when heating demand is below 60%.

REFERENCES

[1] Greenpeace, "China wind power outlook 2012," 2012 [Online]. Available: http://www.gwec.net/wp-content/uploads/2012/11/China-Outlook-2012-EN.pdf
[2] K. Chongqing *et al.*, "Balance of power: Towards a more environmentally friendly, efficient, and effective integration of energy systems in China," *IEEE Power Energy Mag.*, pp. 65–64, Sep./Oct. 2013.
[3] H. Lund, "Electric grid stability and the design of sustainable energy systems," *Int. J. Sustain. Energy*, vol. 24, no. 1, pp. 45–54, Mar. 2005.
[4] "State of Green company," [Online]. Available: https://www.stateofgreen.com/en/Profiles/Ramboll/Products/Heat-Accumulator-for-CHP-plants
[5] V. Vittorio and C. Francesco, "Primary energy savings through thermal storage in district heating networks," *Energy*, vol. 36, no. 7, pp. 4278–4286, Jul. 2011.
[6] Y. H. Zurigat, K. J. Maloney, and A. J. Ghajar, "A comparison study of one-dimensional models for stratified thermal storage tanks," *J. Solar Energy Eng.*, vol. 111, no. 3, 1989.
[7] K. A. R. Ismail, J. F. B. Leal, and M. A. Zanardi, "Models of liquid storage tanks," *Energy*, vol. 22, no. 8, pp. 805–815, Aug. 1997.
[8] H. Lund, E. Münster, and L. H. Tambjerg, "EnergyPlan, computer model for energy system analysis version 6.0," Dept. Development and Planning, Aalborg Univ., Aalborg, Denmark, 2004 [Online]. Available: http://www.plan.aau.dk/GetAsset.action?contentId=3592310&assetId=3614794
[9] D. Connolly, H. Lund, B. V. Mathiesen, and M. Leahy, "A review of computer tools for analyzing the integration of renewable energy into various energy systems," *Appl. Energy*, vol. 87, no. 4, pp. 1059–1082, Apr. 2010.
[10] L. Hong, H. Lund, and B. Möller, "The importance of flexible power plant operation for Jiangsu's wind integration," *Energy*, vol. 41, no. 1, pp. 499–507, May 2012.
[11] W. Liu, W. Hu, H. Lund, and Z. Chen, "Electric vehicles and large-scale integration of wind power—the case of Inner Mongolia in China," *Appl. Energy*, vol. 104, pp. 445–456, Apr. 2013.
[12] M. F. J. Bos, R. J. L. Beune, and R. A. M. Van Amerongen, "On the incorporation of a heat storage device in Lagrangian relaxation based algorithms for unit commitment," *Int. J. Electr. Power Energy Syst.*, vol. 18, no. 4, pp. 207–214, May 1996.
[13] A. Rong, R. Lahdelma, and P. B. Luh, "Lagrangian relaxation based algorithm for trigeneration planning with storages," *Eur. J. Oper. Res.*, vol. 188, no. 1, pp. 240–257, Jul. 2008.
[14] R. Lahdelma and H. Hakonen, "An efficient linear programming algorithm for combined heat and power production," *Eur. J. Oper. Res.*, vol. 148, no. 1, pp. 141–151, Jan. 2003.
[15] P. S. Rao, "Combined heat and power economic dispatch: a direct solution," *Electr. Power Compon. Syst.*, vol. 34, no. 9, pp. 1043–1056, Jan. 2006.
[16] S. Fabricio and P. Pedrero, "Short-term operation planning on cogeneration systems: A survey," *Electr. Power Syst. Res.*, vol. 78, no. 5, pp. 835–848, May 2008.
[17] B. Zeljko and D. Kopjar, "Improvement of the cogeneration plant economy by using heat accumulator," *Energy*, vol. 31, no. 13, pp. 2285–2292, Oct. 2006.

[18] R. Björn, "Combined heat-and-power plants and district heating in a deregulated electricity market," *Appl. Energy*, vol. 78, no. 1, pp. 37–52, May 2004.
[19] P. Meibom, J. Kiviluoma, R. Barth, and H. Brand, "Value of electric heat boilers and heat pumps for wind power integration," *Wind Energy*, vol. 10, no. 4, pp. 321–337, Aug. 2007.
[20] H. Lund, "Large-scale integration of wind power into different energy systems," *Energy*, vol. 30, no. 13, pp. 2402–2412, Oct. 2005.
[21] C. Gianfranco and P. Mancarella, "Distributed multi-generation: a comprehensive view," *Renewable Sustain. Energy Rev.*, vol. 13, no. 3, pp. 535–551, Apr. 2009.
[22] H. Lund, A. N. Andersen, P. A. Østergaard, B. V. Mathiesen, and D. Connolly, "From electricity smart grids to smart energy systems—a market operation based approach and understanding," *Energy*, vol. 42, no. 1, pp. 96–102, Jun. 2012.
[23] A. N. Andersen and H. Lund, "New CHP partnerships offering balancing of fluctuating renewable electricity productions," *J. Cleaner Prod.*, vol. 15, no. 3, pp. 288–293, 2007.
[24] H. Lund and A. N. Andersen, "Optimal designs of small CHP plants in a market with fluctuating electricity prices," *Energy Conv. Manag.*, vol. 46, no. 6, pp. 893–904, Apr. 2005.
[25] F. J. Rooijers and R. A. M. Van Amerongen, "Static economic dispatch for co- generation systems," *IEEE Trans. Power Syst.*, vol. 9, no. 3, pp. 1392–1398, 1994.
[26] R. Jiang, J. Wang, and Y. Guan, "Robust unit commitment with wind power and pumped storage hydro," *IEEE Trans. Power Syst.*, vol. 27, no. 2, pp. 800–810, May 2012.
[27] Illinois Inst. Technol., "Test data," [Online]. Available: http://motor.ece.iit.edu/data/6bus_Data_DR.pdf
[28] R. Aiying and R. Lahdelma, "An effective heuristic for combined heat-and-power production planning with power ramp constraints," *Appl. Energy*, vol. 84, no. 3, pp. 307–325, 2007.
[29] M. B. McElroy, X. Lu, C. P. Nielsen, and Y. Wang, "Potential for Wind Generated Electricity in China," *Sci.*, vol. 325, no. 5946, pp. 1378–1380, 2009.
[30] M. M. Rienecker, M. J. Suarez, R. Todling, J. Bacmeister, L. Takacs, H.-C Liu, W. Gu, M. Sienkiewicz, R. D. Koster, R. Gelaro, I. Stajner, and J. E. Nielsen*, The GEOS-5 Data Assimilation System-Documentation of Versions 5.0.1, 5.1.0, and 5.2.0.* Washington, DC, USA: NASA, 2007, p. 118.
[31] "State electricity regulatory commission China power generation general letter," Beijing, China, 2010.

Xinyu Chen (S'10) received the B.Sc. and Ph.D. degrees from in electrical engineering from Tsinghua University, Beijing, China, in 2009 and 2014, respectively.

He is currently a Research Associate jointly with Tsinghua University and Harvard University. His research interests include load forecasting, smart grid, and wind power integration.

Chongqing Kang (M'01–SM'07) received the Ph.D. degree from in electrical engineering from Tsinghua University, Beijing, China, in 1997.

He is now a Professor with Tsinghua University, Beijing, China. His research interests include renewable energy, power system load forecasting, low-carbon electricity and power system planning and operation.

Mark O'Malley (F'07) received the B.E. and Ph.D. degrees from University College Dublin, Dublin, Ireland, in 1983 and 1987, respectively.

He is a Professor of electrical engineering with University College Dublin, Dublin, Ireland, and Director of the Electricity Research Centre and the Energy Institute.

Qing Xia (M'01–SM'08) received the Ph.D. degree from in electrical engineering from Tsinghua University, Beijing, China, in 1989.

He is now a Professor with Tsinghua University, Beijing, China. His research interests are mainly in power economics, power market, generation and transmission expansion planning, power system reliability, optimization application in power systems, and smart grid.

Jianhua Bai is a Senior Engineer with the State Grid Energy Research Institute, Beijing, China. His research interests are mainly in energy and power system planning.

Chun Liu is a Senior Engineer with Chinese EPRI, Beijing, China. His research interests are mainly in power system dispatch and wind power integration.

Rongfu Sun is a Senior Engineer with Jibei Power Company, State Grid Corporation of China, Beijing, China. His research interests are mainly in wind power integration and power system dispatch.

Weizhou Wang is a Senior Engineer with Gansu Electric Power Research Institute, Lanzhou, China. His research interests are mainly in power system planning and operation.

Hui Li is a Senior Engineer with the State Power Economic Research Institute, Beijing, China. His research interests are mainly in power system planning.